Novel chromosomal imbalances in mantle cell lymphoma detected by genome-wide array-based comparative genomic hybridization

Margit Schraders, Rolph Pfundt, Huub M. P. Straatman, Irene M. Janssen, Ad Geurts van Kessel, Eric F. P. M. Schoenmakers, Johan H. J. M. van Krieken, and Patricia J. T. A. Groenen

Mantle cell lymphoma (MCL) is an aggressive, highly proliferative B-cell non-Hodgkin lymphoma, characterized by the specific t(11;14)(q13;q32) translocation. It is well established that this translocation alone is not sufficient to promote MCL development, but that additional genetic changes are essential for malignant transformation. We have identified such additional tumorigenic triggers in MCL tumors, by applying genome-wide array-based comparative genomic hybridization with an 800-kilobase (kb) resolution. This strategy, combined with a newly developed statistical approach, enabled us to confirm previously reported genomic alterations such as loss of 1p, 6q, 11q, 13q and gain of 3q and 8q, but it also facilitated the detection of novel recurrent genomic imbalances, such as gain of 4p12-13 and loss of 20p12.1-12.3, 20q12-13.2, 22q12.1-12.3, and 22q13.31-13.32. Genomic hotspot detection allowed for the identification of small genomic intervals that are frequently affected (57%-93%), resulting in interesting positional candidate genes such as *KITLG*, *GPC5*, and *ING1*. Finally, by assessing multiple biopsies from the same patient, we show that seemingly stable genomes do show subtle genomic changes over time. The follow-up of multiple biopsies of patients with MCL by high-resolution genomic profiling is expected to provide us with new clues regarding the relation between clinical outcome and in vivo cytogenetic evolution. (Blood. 2005;105:1686-1693)

Introduction

Mantle cell lymphoma (MCL) is a malignant lymphoproliferative disorder, which accounts for 6% of all non-Hodgkin lymphomas.[1,2] It is characterized by the specific t(11;14)(q13;q32) translocation, which juxtaposes the cyclin D1 gene to the immunoglobulin heavy chain junctional region, resulting in the overexpression of cyclin D1.[3-5] The overexpression of cyclin D1 is assumed to play an important role in lymphomagenesis since it is involved in the cell cycle regulation at the G_1 to S transition phase.[6,7] Transgenic mice models, however, have shown that overexpression of cyclin D1 alone is not sufficient to trigger lymphoma development, but that additional genetic changes are necessary for the malignant transformation of MCL.[8,9] Indeed, MCLs are cytogenetically unstable, but it is currently unknown which genes are selectively deregulated due to this instability. It is also not known whether additional relevant gene alterations occur, which determine the progression of the disease.

In the past, several groups have systematically investigated the presence of recurrent cytogenetic anomalies in MCL cases by conventional comparative genomic hybridization (CGH).[10-14] The search for genes that might be causally related to malignant transformation of MCL, however, is hampered by the fact that conventional CGH provides only limited resolution: even the smallest possible unbalanced region detected by chromosomal CGH (about 3 Mb) is likely to contain an amount of genes exceeding the number manageable in standard positional functional candidate approaches.[15,16]

The aim of this study was to identify gains and losses of chromosomal regions in MCL at a higher resolution than can be obtained with conventional CGH. To this end, we have used microarray-based comparative genomic hybridization (array-CGH) using DNA chips containing a triplicate of 3565 clones mapping at evenly spaced intervals throughout the entire genome to detect cytogenetic anomalies at high resolution.[17-19] Very recently, the power of this array-based approach in the detection of chromosomal aberrations in MCL (cell lines) has been shown in 2 very elegant studies. Kohlhammer et al[20] described the analysis samples from patients with MCL by using a DNA array containing 513 clones, covering regions known to be recurrently affected in MCL or containing oncogenes or tumor suppressor genes, and an additional 209 clones covering the genome with a 15-Mb resolution. This approach facilitated the refinement of the chromosomal imbalances previously described in conventional CGH studies and enabled them to identify a number of novel consensus regions. In addition, DeLeeuw et al[21] have fully exploited the strongly enhanced resolution offered by array-CGH and showed that the use of a high-resolution array indeed facilitates the identification of candidate genes in a panel of 8 MCL-derived cell lines. Using a DNA microarray of 32 433 clones spanning the entire human genome, they identified several positional candidate genes in 8 commonly used MCL cell lines. In our study we describe the molecular cytogenetic characterization of 17 MCL tumor samples using an

From the Departments of Pathology, Human Genetics, and Epidemiology and Biostatistics, University Medical Centre Nijmegen, Nijmegen, The Netherlands.

Submitted July 16, 2004; accepted September 30, 2004. Prepublished online as *Blood* First Edition Paper, October 21, 2004; DOI 10.1182/blood-2004-07-2730.

Support was obtained from the European Union for the European Mantle Cell Lymphoma Network (FP6).

M.S. and R.P. contributed equally to this work.

Reprints: Margit Schraders, Department of Pathology, University Medical Centre Nijmegen, PO Box 9101, 6500 HB Nijmegen, The Netherlands; e-mail: m.schraders@pathol.umcn.nl.

The publication costs of this article were defrayed in part by page charge payment. Therefore, and solely to indicate this fact, this article is hereby marked "advertisement" in accordance with 18 U.S.C. section 1734.

unbiased genome-wide DNA array providing an 800-kilobase (kb) resolution.

Although performing successful array-CGH hybridizations in a reproducible manner is certainly not a triviality, generating huge amounts of data with genome-wide array-based CGH is relatively straightforward. Just like in expression-profiling approaches, a big challenge lies in developing robust statistical methods to analyze this large amount of data and to reliably identify the most recurrent chromosomal imbalances. In this context, we developed a novel statistical approach that enabled us to confirm chromosomal imbalances previously described in MCL. And, more importantly, the approach enabled us to identify novel genetic regions of interest. New chromosomal intervals that were identified in our study include gain of 4p12-13 and loss of 20p12.1-12.3, 20q12-13.12, 22q12.1-12.3, and 22q13.31-13.32. Several candidate genes were identified through the detection of very small chromosomal regions that showed copy number gain or loss in at least 57% (and up to 93%) of the tumor specimens investigated. In addition, we studied the occurrence of additional chromosomal imbalances during disease progression by analyzing a primary tumor and subsequent relapses.

Patients, materials, and methods

Patients

MCL cases included in our study were confirmed on the basis of histology and immunophenotype. Cyclin D1 overexpression was detected in all cases except case MC25. Case MC25 did contain the t(11;14)(q13;q32), as it was confirmed by fluorescence in situ hybridization (FISH) analysis. All cases were diagnosed as classical MCL, with a tumor load above 90%. In total 17 tumor specimens from 14 patients were included in our study (10 men, 4 women; aged 49-82 years; mean, 62 years). Four of the specimens were derived from 1 patient, this included material from the primary tumor (MC50) and from subsequent relapses (MC51-MC53) over 8 years. The clonal relationship of these samples was demonstrated by identical rearrangements of the *IGH* immunoglobulin gene (data not shown). Approval for these studies was obtained from the institutional review board. Informed consent was provided according to the Declaration of Helsinki.

Extraction of genomic DNA was performed on whole frozen sections according to standard procedures using proteinase K digestion and NaCl precipitation. The DNA was further purified using the QIAamp DNA mini kit (Qiagen, Hilden, Germany) according to the manufacturer's protocol.

Array-based CGH

Array-based CGH was performed using a microarray containing a total of 3565 colony-purified FISH-verified and phage-tested bacterial artificial chromosome (BAC) clones, including approximately 3200 clones obtained through a collaboration with the Children's Hospital Oakland Research Institute, BACPAC Resources (Oakland, CA), and other groups, to cover the genome with a 800-kb resolution.[19] This 3200-clone set represents a subset of the larger 7.6-k (8.9-k) set that has previously been described by Cheung et al[19] and contains all 7600- (8900-) clone sets, which are currently being distributed as FISH-verified clones by BACPAC Resources (http://bacpac.chori.org/). In addition to this set of clones, the BAC array contained a higher clone density in subtelomeric regions as well as on chromosomes 12 and 18, through the addition of clones used in previous studies.[22-24] This array has been extensively validated for the detection of copy number alterations using normal versus normal control experiments, including sex mismatches, as well as experiments in which cases with known microdeletion syndromes were tested.[25] To facilitate a quick scan regarding experimental performance of individual samples, all hybridizations were performed in a sex-mismatch fashion. Preparation of BAC arrays, labeling, and hybridizations were performed essentially as described by Vissers et al.[25] All hybridizations were performed on the same batch of arrays, thereby excluding minor batch-to-batch differences.

Analysis of the microarray images was performed using the software package GenePix Pro 4.0 (Axon Instruments, Foster City, CA). For each spot the median pixel intensity minus the median local background for both dyes was used to obtain a genomic copy number ratio. Data normalization was performed by using the software package SAS version 8.0 (SAS Institute, Cary, NC) per array subgrid by applying linear regression with the $\log_2$ transformed test over reference value (T/R) and the average logarithmic fluorescent intensities. All mapping information regarding clone locations, cytogenetic bands, and the genomic contents was retrieved from the University of California Santa Cruz (UCSC) genome browser (April 2003 freeze).

Development of a moving average algorithm for the detection of genomic imbalances

Due to several reasons, array data can be very hard to interpret (eg, clone mapping errors, clone performance, spotting quality and experimental noise). Especially the identification of contiguous clone stretches that represent areas of genomic loss or gain is not a sinecure. To minimize these potential problems and to judge the data of each slide at its own quality level, we have developed an algorithm that is based on extreme values of moving averages (MAs; an approach that is commonly used for the detection/prediction of index trends in the context of stock market developments) of normalized $\log_2$ ratios with different window sizes. By using this algorithm the noise of a slide becomes of less importance and stretches of clones with relatively extreme high- or low-average signal ratios can be automatically identified. In the first step of the data the clones are shuffled in random order, this is done 50 times, thereby resulting in 50 data sets of each array. For each data set the moving average with window width from 2 to 10 is calculated. This means the average $\log_2$ ratio is calculated for clones 1 and 2, 2 and 3, 3 and 4, and so forth. The same is done for 3 to 10 neighboring clones. The maximum and minimum values of the moving averages over the shuffled array for each window width are calculated, leading to maximum and minimum averages of 2 clones, 3 clones, and so forth. In the second step, the most extreme values are identified and used as the thresholds. In the third step the maxima and the minima for the moving averages with window width 2 to 10 are calculated for the unshuffled, or the original, array. When these average $\log_2$ ratios exceed the thresholds, they are considered as extreme moving averages and therefore as a consecutive area of nonoverlapping up- and down-regulated consecutive clones. The same procedure is used for moving averages with window widths from 11 to 30. As the algorithm only detects the most extreme gains and losses, careful inspection of the normalized values was necessary to merge nearby gains or losses into 1 consecutive area. Chromosomes X and Y were not included in this analysis. Mathematical and statistical details underlying this algorithm are available on request (h.straatman@epib.kun.nl).

Genomic hotspot detection

Analysis of the data was performed to detect hotspots of genomic imbalances. First of all, suspicious clones, which are defined as clones that have either a standard deviation more than 0.26 or less than 0.026 or a z value (average ratio divided by standard error) more than 5 in the normal-versus-normal hybridizations, were identified. In addition, clones were excluded that showed a standard deviation more than 0.3 over triplicates in the individual experiments, as well as clones with fewer than 2 replicates remaining after this analysis. "Hotspots" were defined as clones with a $\log_2$ (test over reference) ratio more than 0.3 or less than -0.3 in 8 or more cases. These boundaries were chosen by examining the results of the normal-versus-normal hybridizations and the results of previously published work.[17,23,25] As MC50 to MC53 were derived from the same patient, only the primary tumor (MC50) was considered in this analysis. Chromosomes X and Y were not included in this analysis.

Results

Recurrent genomic imbalances found in MCL

Array-based CGH allows detection of losses and gains of subtle as well as gross chromosomal intervals. All MCL cases were found to harbor multiple copy number changes, although some cases showed a more complex genomic profile than others. To identify the recurrent genomic imbalances in the MCL cases, consecutive areas of gain or loss were determined with the algorithm previously described. The behavior of individual clones was tested by performing 4 normal-versus-normal hybridizations with genomic DNA derived from normal healthy blood donors. The moving average algorithm, as described in "Patients, materials, and methods," was used to detect stretches of consecutive clones with aberrant average ratios, indicating gain or loss of chromosomal interval. When this algorithm was used in the 4 normal-versus-normal hybridizations, only 2 extreme moving averages above 0.3 or below −0.3 were found; 1 with a mean of −0.81 and window width 2, and 1 with a mean of 0.36 with a window width 3. The most extreme moving averages with window width 11 to 30 were all within the "normal" −0.2 to 0.2 range. In patient material the most extreme moving averages are in all cases above 0.2 or below −0.2.

We will describe the most recurrent genomic imbalances observed in our MCL series. Chromosomes with a high number of gains or losses are depicted in Figures 1 and 2. The minimal overlapping regions were determined by assessing the smallest region of deletion (or gain) overlap in at least 5 patients and detailed descriptions of megabase (Mb) positions and flanking clones are listed in Table 1. The moving average algorithm enabled us to identify consecutive areas of gains or loss, which confirm, and for some loci refine, a number of genomic alterations previously described in MCL. In total 216 consecutive areas were identified in 14 patients, varying from 9 to 27 consecutive areas per case and an average value of 15.4 consecutive areas per case. Loss within chromosome 1p (Figure 1A) was seen in 71% of the cases, with a minimal overlapping region at 1p22.1 to 31.1. Gain of 3q was present in 64% of the cases (Figure 1B). Although the aberrations appeared to be dispersed over the entire chromosome arm, 2 minimal overlapping regions could be identified, 3q13.13 to 21.1 and 3q25.32 to 26.2. Deletions of 6q were found in 36% of the cases: all showed loss of 6q23.2-27. Six cases showed gain of 8q, overall the whole chromosome was affected. Two minimal overlapping regions were identified though, namely 8q21.11-21.3 and 8q23.1-23.3 (Figure 1C). In addition, a deletion of chromosome 10q was found in 36% of the cases, and mainly involved 10q26.13-26.2. Chromosome 11 (Figure 1D) showed a particularly interesting pattern: 8 cases (57%) showed loss of 11q22.3-23.3, whereas 4 cases (29%) showed gain of 11p12-q11. Chromosome 13 (Figure 1E) showed losses within 13q in 57% of the cases: 2 minimal regions were determined 13q12.3-14.31 and 13q31.3-33.2. Note that copy number gains of partly overlapping regions of chromosome 13q were also seen in 4 cases.

The moving average algorithm also allowed for the detection of new recurrent genomic imbalances not reported before. A novel finding was gain of chromosome 4p, which was present in 57% of the cases in our study with a minimal overlapping region of 4p12-13 (Figure 2A). Another novel finding is losses on chromosome 20; the first minimal overlapping region is 20p12.1-12.3, which is present in 43% of the cases, and the second minimal overlapping region is 20q12-13.12, which was also present in 43% of the cases. Finally, loss of chromosome 22q (Figure 2C) was seen in 79% cases. Two minimal overlapping regions are 22q12.1-12.3 and 22q13.31-13.32. MC25 showed an interesting pattern within 22q: 2 regions showed copy number loss and 1 region lying in between showed copy number gain.

The chromosomes shown in Figures 1 and 2 contain many imbalances, whereas other chromosomes seem to be relatively stable. On chromosome 2, for example, no consecutive areas were found in any of the cases. Chromosomes 5, 7, 14 to 18, and 21 show only few consecutive areas. Loss of 9p was seen in 3 (21%) of 14 cases, while gain of 9p was also detected in 3 other cases in our study. Interestingly, chromosome 19 was affected in only 2 cases, but they all showed a very large consecutive area, comprising 19p13.3-19q13.12.

Genomic evolution during recurrent disease

As shown in Figure 3, the genomic profiles of the primary tumor (MC50) and subsequent relapses (MC51-MC53) at first sight appeared to be very similar. However, careful examination of the normalized values of the consecutive areas of gain or loss in these cases shows that there indeed are subtle differences as can be noted in Figures 1 and 2. When a consecutive area of gain or loss was

Table 1. Minimal common regions found in MCL

Chromosome	Gain or loss	Upper flanking clone	Lower flanking clone	Mb region	Chromosome region	Incidence, %
1	Loss	RP11-246o4	RP11-89b24	82,16-94,06	1p22.1-31.1	50
3	Gain	RP11-89e20	RP11-79m2	111,56-124,32	3q13.13-21.1	36
3	Gain	RP11-89f24	RP11-24116	158,78-170,33	3q25.32-26.2	50
4	Gain	RP11-90d3	RP11-90f11	43,04-47,61	4p12-13	57
6	Loss	RP11-54p6	RP11-81h13	133,52-167,42	6q23.2-27	36
8	Gain	RP11-93j13	RP11-90g19	77,53-90,20	8q21.11-21.3	36
8	Gain	RP11-79o20	RP11-21j16	109,25-117,80	8q23.1-23.3	36
10	Loss	RP11-255d5	RP11-5m6	123,71-127,89	10q26.13-26.2	36
11	Loss	RP11-262j9	RP11-279m1	110,51-114,30	11q22.3-23.3	57
13	Loss	RP11-90m5	RP11-487o12	27,75-46,16	13q12.3-14.31	43
13	Loss	RP11-100a3	RP11-29b2	93,16-104,06	13q31.3-33.2	43
20	Loss	RP11-103h2	RP11-238i2	8,74-14,42	20p12.1-12.3	43
20	Loss	RP11-93119	RP11-169a6	38,89-45,58	20q12-13.12	43
22	Loss	RP11-91k24	RP11-5i24	24,95-33,34	22q12.1-12.3	50
22	Loss	RP11-1064g15	RP11-629g24	45,82-46,90	22q13.31-13.32	50

Mb positions and chromosome bands of the clones were determined with the USSC genome browser (April 2003 freeze). Minimal common regions were determined by identifying the smallest region of overlap in the consecutive areas of the different cases.

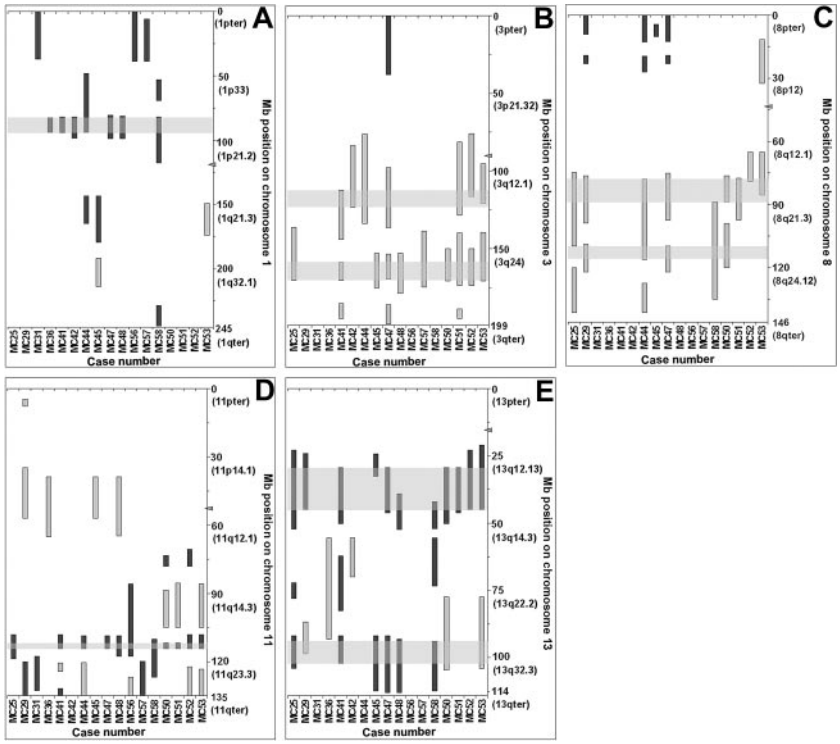

Figure 1. Schematic representation of the chromosomal imbalances previously reported in classic CGH studies. Gains are shown in light gray and losses in dark gray. The centromere is represented by an arrowhead. MB positions and chromosome bands were determined with the UCSC genome browser (April 2003 freeze). When consecutive areas of the same case were less then 5 BAC clones apart and these clones had a mean similar to the mean of the consecutive areas, they were combined in 1 consecutive area. The most overlapping aberrations were loss of 1p, 11q, 13q, plus gain of 3q and 8q.

present in 1 or more of the samples, usually a gain or loss was observed in the same region of the other samples. However, several changes in the consecutive areas of these samples were identified that showed an intriguing difference: MC53, the third relapse, showed gain of 1q21.3-25.2, while the primary tumor and subsequent relapses showed no abnormalities in this region (Figure 1A). MC50 does not show loss of the 11qter region, while this is present in the relapses. Another difference is the presence of gain of 9p in MC50, which is not present in any of the relapses. Hence, it seems that, although the recurrent lymphomas of this patient appear genetically stable, several genetic alterations occur in the course of the disease.

Do typical MCL cases represent a homogenous group?

We investigated the possibility to subcategorize our group of mantle cell lymphoma cases into clearly distinguished subgroups. For this purpose we made use of a software package called "Gene Cluster" written by Michael Eisen.[26] Clustering was performed on 2 data sets. The first set contained all the clones on the BAC array, and the second set contained clones involved in the consecutive areas found with the moving average. With the 2 data sets used no subgroups could be identified, the cases all clustered together with 2 exceptions, namely MC25 and MC58. MC25 showed few chromosomal imbalances and is derived from the spleen, while the other cases were all located in lymph nodes. Case 58 contained many chromosomal imbalances, but there is no apparent reason why this 1 case does not cluster together with the other cases. Interestingly, MC50 to MC53 grouped together as could be expected since they were all derived from the same patient.

Genomic hotspots in MCL

The smallest regions of overlap as determined from the consecutive areas still contain many positional candidate genes that might be involved in the development of MCL. One of the advantages of array-based CGH is the high resolution of copy-number screening; therefore the detection of very small areas consisting of a single clone (hotspots) was used to narrow down the amount of potentially causative genes. Genomic hotspots derived in this way are listed in Tables 2 and 3. In total 28 hotspots with copy number gain and 21 hotspots with copy number loss were identified, with an average of 17.8 and 12.9 per case, respectively. An intriguing observation is that certain chromosomal areas contain multiple

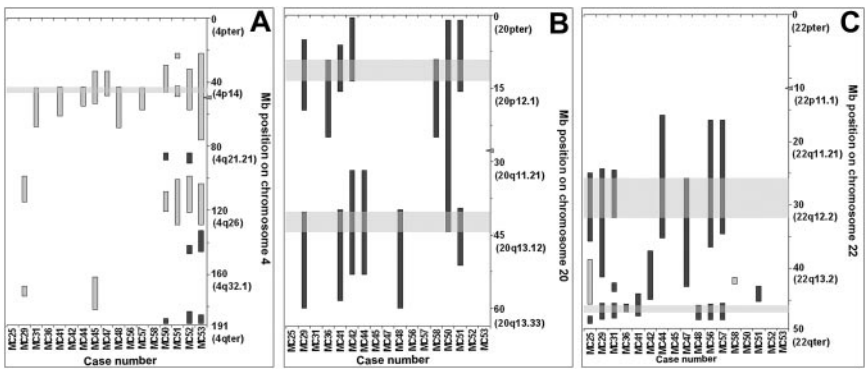

Figure 2. Schematic representation of novel chromosomal imbalances in MCL cases. Gains are shown in light gray and losses in dark gray. The centromere is represented by an arrowhead. MB positions and chromosome bands were determined with the UCSC genome browser (April 2003 freeze). When consecutive areas of the same case were less than 5 BAC clones apart and these clones had a mean similar to the mean of the consecutive areas, they were combined in 1 consecutive area. The minimal overlapping regions identified in these chromosomes are 4p12-13, 20p12.1-12.3, 20q12-13.12, 22q12.1-12.3, and 22q13.31-13.32.

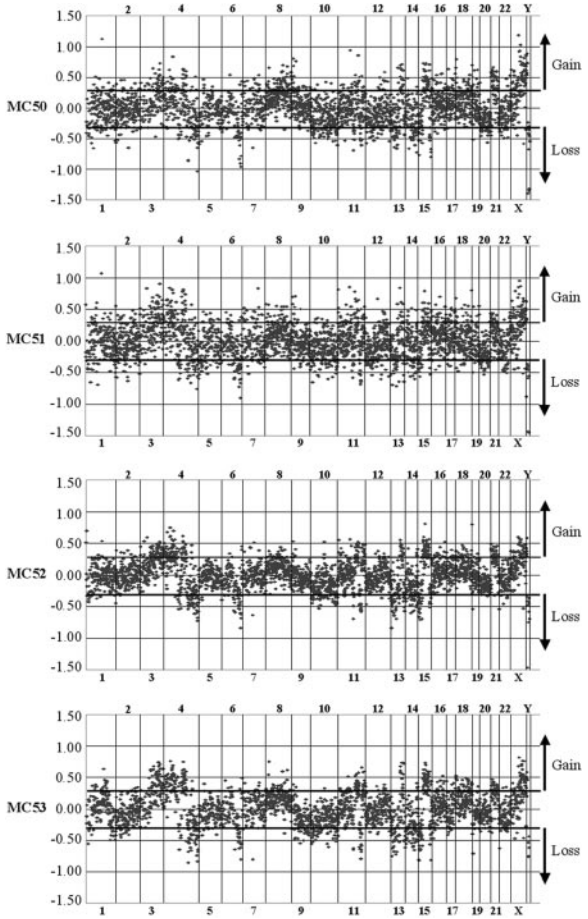

Figure 3. Genomic profiles of MCL cases. Data are plotted as the mean $\log_2$ ratios over reference ratios. BACS are ordered by position over the genome from 1 to Y. BAC positions were determined with the UCSC genome browser (April 2003 freeze). The primary tumor (MC50) and subsequent relapses (MC51-MC53) from the same patient show a similar genomic profile.

hotspots. Chromosome 1, for instance, contains 2 hotspots that are very close together, RP11-2p11 and RP11-79d15. Analysis of the hybridization data revealed that there is 1 clone lying in between (RP11-265f14); however this clone unfortunately was not informative in our patient samples. Therefore, we speculate that these hotspots represent a consecutive area of loss in MCL involving 1p36.13-p36.21. Other consecutive clones that show copy number loss are RP11-19j14 and RP11-122a8 on chromosome 13, which represent loss of 13q32.2-q32.3, and RP11-3p8 and RP11-19o15, which represent loss of 13q34. Consecutive clones that show copy number gain are RP11-79f11 and RP11-91f17 at 3q26.1 and RP11-89i16 and RP11-21j16 at 8q23.3. Especially, copy number gain of consecutive clones RP11-88n10 and CTD-2101j13 at 12q32-q32.3 is of great interest since this gain area was found in 93% of the MCL cases.

Discussion

Besides the specific t(11;14)(q13;q32) translocation, which is generally accepted as being the primary tumorigenic trigger in MCL development, additional genetic changes appear to be essential for development and progression of MCL.[3-5,8] To identify these subsequent genetic alterations, several groups have successfully used conventional comparative genomic hybridization to identify chromosomal regions with aberrant copy number.[10-14] In this study we describe the use of genome-wide array-based CGH in combination with a novel and extensive statistical (moving average) approach for the detection of consecutive areas of chromosomal imbalances in MCL.

Chromosomal imbalances that have previously been described in all of the conventional CGH studies are gains of 3q and 8q and losses of 1p, 6q, 11q, and 13q, all of which were confirmed in this study. The minimal overlapping regions found within the consecutive chromosomal areas in our study are all mapping within the cytogenetic intervals that were previously identified by others.[10-14] Our studies not only allowed for a molecular definition of these intervals, but also allowed further refinements of these areas to be achieved due to the high resolution of the array-based CGH approach.

In addition to the improved definition of previously identified cytogenetic intervals, we identified novel chromosomal regions involved in MCL. Chromosomes 20 and 22 represent 2 of the smallest chromosomes and are therefore difficult to assess with conventional CGH. Our results clearly show that this limitation can readily be overcome by array-based CGH: we identified 2 minimal overlapping regions on chromosome 20 that showed copy number loss, located at 20p12.1-12.2 and 20q12-13.2. Loss of chromosome 22q was detected in 79% of the cases with 2 minimal overlapping regions, 22q12.1-12.3 and 22q13.31-13.32, respectively. Another big advantage of array-based CGH compared with conventional CGH is the detection of subtle changes located at the subtelomeric regions, as is illustrated by the involvement of the 2q37.2 region that was identified as a hotspot with copy number loss in 62% of the cases in this study.

Very recently, impressive work has been published describing the use of CGH-array to identify chromosomal imbalances in tumor specimens of MCL cases, or MCL-derived cell lines.[20,21] Using a microarray of 32 433 clones spanning the human genome at high resolution, DeLeeuw et al[21] analyzed 8 MCL cell lines to determine whether these adequately represent MCL. This powerful approach enabled them to perform whole genome analysis and to identify novel genetic alterations in these cell lines. Although of considerable interest, data from this study are not necessarily comparable to the in vivo cytogenetic anomalies present in MCL tumor samples, as these (sometimes high passage number) cell lines can be considered as clonal expansions of only a subset of the tumor cells, on which the selective pressure applied by the specific culturing conditions is likely to not reflect in vivo selective mechanisms. Kohlhammer et al[20] investigated the chromosomal imbalances by using the DNA-chip technology in MCL tumor specimens. The array they used was composed of 513 clones covering regions, which were already known to be recurrently affected in MCL or containing oncogenes or tumor suppressor genes, and was further enriched by the addition of 209 clones covering the genome with a 15-Mb resolution.[20] This array allowed for the identification of a number of interesting consensus regions of gain or loss in MCL tumors. With our unbiased 3.6-k array, we were able to confirm the chromosomal imbalances found by Kohlhammer et al.[20] It should be noted that not all of these areas are listed in Table 1, since we included solely the genomic anomalies present in at least 36% of the cases. Due to our unbiased approach, the high resolution and the overall performance of our genome-wide array and the new statistical method of detection of consecutive areas, we were able to further refine these areas of interest and to identify novel areas of interest as well. Some of the genomic aberrations may have prognostic relevance, as has previously been

Table 2. Most frequently gained clones in MCL

Clone name	Base position, Kb	Cytogenetic band	% of cases with copy number gain	Genes in affected interval
Group A				
RP11-79f11*	Chr3:165,285	3q26.1	83	*SI, BCHE*
RP11-21j16	Chr8:116,016	8q23.3	77	*TRPS1*
RP11-90m7	Chr3:164,334	3q26.1	75	—
RP11-80f24	Chr8:78,335	8q21.12	69	—
RP11-89i16	Chr8:114,648	8q23.3	69	—
RP11-90d3	Chr4:43,447	4p13	64	—
RP11-89e20	Chr3:112,456	3q13.13	64	*PVRL3, CD96, TACTILE*
RP11-91f9	Chr3:119,136	3q13.32	62	—
RP11-91f17	Chr3:167,543	3q26.1	57	*SI, BCHE*
Group B				
RP11-90e13*	Chr4:171,790	4q33	85	—
RP11-54818	Chr12:55,220	12q13.2	75	*NEUROD4, HEM1, DCD*
RP11-75h6	Chr19:0,988	19p13.3	73	*DRIL1, CNN2, STK11*
RP11-91i19	Chr4:144,372	4q31.21	69	*INPP4B, HP43, SNARCA5*
RP11-14k17	Chr11:39,871	11p12	69	—
RP11-111p16	Chr6:55,523	6p12.1	69	*BMP5, COL21A1*
RP11-91o1	Chr13:89,942	13q31.3	69	*GPC5*
RP11-89a6	Chr15:54,253	15q21.3	69	*TCF12, AQP9*
RP11-88n10	Chr12:88,021	12q21.32	67	*KITLG*
CTD-2101j13	Chr12:88,824	12q21.3	64	*DUSP6, TUWD12, KITLG*
RP11-142f22	Chr8:100,581	8q22.2	64	*COX6, RNF19, SPAG1*
RP11-171g12	Chr4:181,787	4q34.3	62	—
RP11-35p16	Chr16:4,580	16p13.3	62	*GLIS2, HMOX2, DNAJA3*
RP11-71f18	Chr7:19,239	7p21.1	62	*HDAC9, TWIST1, FERD3L*
RP11-131k16	Chr4:121,820	4q27	57	*MAD2L1, PRDM5*
Group C				
RP11-91a22	Chr16:46,347	16q11.2	86	*SHCBP1, VPS35, GPT2*
RP11-91m10	Chr11:85,444	11q14.1	77	*DLG2*
RP11-229a12	Chr3:57,333	3p14.3	75	*DNAH12, SLMAP, ARF 4*
RP11-172k14	Chr5:74,567	5q13.3	62	*HEXB, EFG2, POLK, F2R*

In group A, hotspots are present in the smallest regions of overlap. In group B, hotspots are present in consecutive areas. In group C, hotspots are not present in any of the consecutive areas. Mb positions of the clones were determined with USSC genome browser (April 2003 freeze). Hotspots were defined as clones with a ratio >0.3 in 8 or more of the 14 cases. Percentages were calculated by dividing the number of cases with ratio >0.3 with the number of samples that gave a hybridization signal. RP11-79f11 and RP11-91f17, RP11-89i16 and RP11-21j16, RP11-88n10 and CTD-2101j13 are consecutive clones. Genes were identified in the Mb region between the flanking clones of a hotspot.

— indicates that there are no known genes in the interval.

*These clones were identified as polymorphisms in the human genome by either Sebat et al[27] or Iafrate et al.[28]

established for the 13q14.3 deletion.[20] In our analysis, we focused on highly recurrent genomic imbalances and were able to identify very small chromosomal regions with copy number gain or loss by hotspot detection.

One of the genes that has been reported to be involved in the development of MCL is *ATM*.[29,30] This gene is frequently inactivated in MCL by deletion of 1 allele and mutations in the other allele. On the BAC array used for this study, no clones were present that contained the *ATM* gene itself. Interestingly, however, clones flanking this gene were deleted in 7 of 14 cases. In the cases, which do not show loss of this region, we suppose that other genes must have been involved in the development of MCL.

For the more subtle target intervals, high-resolution array-CGH enabled us to identify positional candidate genes that might be involved in the development of MCL, as listed in Tables 2 and 3. Additional studies are needed to validate the possible functional role of their encoded proteins in the context of MCL development. On the basis of the recurrent change in copy number, we expect that the *KITLG* gene could be of great importance. As shown in Table 2, there are 2 BAC clones flanking this gene and a gain of either 1 of these clones was observed in 93% of the MCL tumor samples analyzed. The *KITLG* gene encodes the stem cell factor protein, which is a hematopoietic growth factor and ligand for the c-kit tyrosine kinase receptor (KIT). It has been shown that activating mutations in KIT result in ligand-independent tyrosine kinase activity, autophosphorylation of KIT, uncontrolled cell proliferation, and stimulation of downstream signaling pathways.[31] So, we can hypothesize that overexpression of the *KITLG* gene might lead to continuous activation of KIT and therefore to uncontrolled cell proliferation.

One of the hotspots with copy number gain comprises a genomic interval at 13q31, encompassing the *GPC5* gene. Gain of this gene was also reported by DeLeeuw et al.[21] Previous studies have shown that GPC5 was overexpressed in lymphoma cell lines that had shown amplification, in comparison with those that had not, suggesting that the transcriptional activity of this gene is, at least to some extent, regulated at the gene-dosage level. These findings suggested that *GPC5* is a likely target for amplification of the locus and that overexpression of this gene may contribute to development and/or progression of lymphomas.[32,33] Another candidate gene is *ING1*, which encodes the "inhibitor of growth protein 1." Loss of this region was observed in 75% of the cases. It has been demonstrated that *ING1* can act as a potent growth regulator, which has been proposed to act as candidate tumor suppressor gene whose inactivation may contribute to the development of cancers.[34] In addition, decreased expression of inhibitor of growth mRNA in lymphoid malignancies has previously been reported.[33] Although several potentially important candidate

Table 3. Most frequently lost clones in MCL

Clone name	Base position, Kb	Cytogenetic band	% of cases with copy number loss	Genes in affected interval
Group A				
RP11-89b24	Chr1:94,003	1p22.1	77	*PARG1, TGFBR3, GF11*
RP11-122a8	Chr13:98,597	13q32.3	67	*ZIZIMIN1, STK24, EBI2*
RP11-246o4	Chr1:82,559	1p31.1	62	—
RP11-19j14	Chr13:97,890	13q32.2	62	*FARP1, STK24, DOCK9*
RP11-65f22	Chr22:31,034	22q12.3	62	*SLC5A4, LIF, PES1*
RP11-40h10	Chr13:94,399	13q32.1	57	—
RP11-17i11	Chr13:42,711	13q14.11	57	*DNAJD1, MJC*
Group B				
RP11-58f7*	Chr7:156,972	7q36.3	79	*PTPRN2*
RP11-3p8	Chr13:111,893	13q34	75	*ING1, SOX1*
RP11-88j24	Chr1:36,922	1p34.3	73	*GRIK3*
CTC-200d12*	Chr14:104,922	14q32.33	71	*IGHM*
RP11-19o15	Chr13:112,427	13q34	69	*TUBGCP3*
RP11-58c16	Chr13:50,175	13q14.3	67	*NEK3, CKAP2*
RP11-278e23	Chr22:17,193	22q11.21	64	*DRCR6, ZNF74, HIC2*
RP11-2111	Chr1:14,410	1p36.21	57	*MGC4342*
RP11-2c23	Chr11:20,127	11p15.1	57	*NAV2*
RP11-79d15	Chr1:17,016	1p36.13	57	*PAD12 SDHN, PAX7*
Group C				
RP11-55m23†	Chr1:54,836	1p32.3	77	*BSND*
RP11-116m19	Chr2:236,646	2q37.2	62	*CENTG2, SH3BP4*
RP4-771p4	Chr7:73,000	7q11.23	62	*LIMK, RFC21*
RP11-14k9	Chr5:168,448	5q35.1	62	*SLIT3, RARS, PANK3*

In group A, hotspots are present in the smallest regions of overlap. In group B, hotspots are present in consecutive areas. In group C, hotspots are not present in any of the consecutive areas. Mb positions of the clones were determined with USSC genome browser (April 2003 freeze). Hotspots were defined as clones with a ratio < -0.3 in 8 or more of the 14 cases. Percentages were calculated by dividing the number of cases with ratio < -0.3 with the number of samples that gave a hybridization signal. RP11-19j14 and RP11-122a8, RP11-3p8 and RP11-19o15 are consecutive clones.

— indicates that there are no known genes in the interval.

*These clones were identified as polymorphisms in the human genome by either Sebat et al[27] or Iafrate et al.[28]

†This clone was mapped to different locations using the USSC genome browser; in this table the position in FISH clone track was used for this table. Genes were identified in the Mb region between the flanking clones of a hotspot.

genes were identified during this study, the actual functional role of the products encoded by these genes in MCL development needs further investigation.

Recently, 2 studies have been published describing the occurrence of large-scale polymorphisms in the human genome.[27,28] Iafrate et al[28] investigated the occurrence of large-scale copy-number variations (LCVs) in the human genome by means of array-CGH and identified 255 loci, which showed copy number gain or loss in unrelated healthy individuals. Sebat et al,[27] using a similar approach, identified 76 large-scale copy-number polymorphisms (CNPs) in the human genome. A small number (n = 4) of the clones reported in Tables 2 and 3 were also reported in the context of those studies. However, these clones were involved in much higher percentages in our study, which might be explained by differences in, for instance, a different ethnic background of our sample population. Therefore, we currently believe that copy number changes observed for these particular clones indeed represent genomic polymorphisms, which are not causally related to the onset of the disease. Future research into this matter might provide us with data regarding a possible predisposition effect related to the occurrence of (some of) these polymorphisms.

This study also included a primary MCL and 3 subsequent relapses, all from the same patient. Analysis of the chromosomal imbalances of these samples showed that there was apparent genomic stability, although subtle differences during the course of the disease were found as well. These findings suggest an expansion of a specific subclone from the primary genetically heterogenous MCL tumor during the course of the disease.

In summary, this study demonstrates that array-based CGH is a powerful technique for the detection of chromosomal aberrations at a high resolution. In addition, array-CGH will be a useful tool for assessment of the cytogenetic evolution over time in relation to clinical outcome or response to therapy.

References

1. A clinical evaluation of the International Lymphoma Study Group classification of non-Hodgkin's lymphoma. The Non-Hodgkin's Lymphoma Classification Project. Blood. 1997;89:3909-3918.
2. Anderson JR, Armitage JO, Weisenburger DD. Epidemiology of the non-Hodgkin's lymphomas: distributions of the major subtypes differ by geographic locations. Non-Hodgkin's Lymphoma Classification Project. Ann Oncol. 1998;9:717-720.
3. Tsujimoto Y, Jaffe E, Cossman J, et al. Clustering of breakpoints on chromosome 11 in human B-cell neoplasms with the t(11;14) chromosome translocation. Nature. 1985;315:340-343.
4. Erikson J, Finan J, Tsujimoto Y, Nowell PC, Croce CM. The chromosome 14 breakpoint in neoplastic B cells with the t(11;14) translocation involves the immunoglobulin heavy chain locus. Proc Natl Acad Sci U S A. 1984;81:4144-4148.
5. Tsujimoto Y, Finger LR, Yunis J, Nowell PC, Croce CM. Cloning of the chromosome breakpoint of neoplastic B cells with the t(14;18) chromosome translocation. Science. 1984;226:1097-1099.
6. Baldin V, Lukas J, Marcote MJ, Pagano M, Draetta G. Cyclin D1 is a nuclear protein required for cell cycle progression in G1. Genes Dev. 1993;7:812-821.
7. Bosch F, Jares P, Campo E, et al. PRAD-1/cyclin D1 gene overexpression in chronic lymphoproliferative disorders: a highly specific marker of mantle cell lymphoma. Blood. 1994;84:2726-2732.

8. Lovec H, Grzeschiczek A, Kowalski MB, Moroy T. Cyclin D1/bcl-1 cooperates with myc genes in the generation of B-cell lymphoma in transgenic mice. EMBO J. 1994;13:3487-3495.
9. Bodrug SE, Warner BJ, Bath ML, et al. Cyclin D1 transgene impedes lymphocyte maturation and collaborates in lymphomagenesis with the myc gene. EMBO J. 1994;13:2124-2130.
10. Allen JE, Hough RE, Goepel JR, et al. Identification of novel regions of amplification and deletion within mantle cell lymphoma DNA by comparative genomic hybridization. Br J Haematol. 2002;116: 291-298.
11. Martinez-Climent JA, Vizcarra E, Sanchez D, et al. Loss of a novel tumor suppressor gene locus at chromosome 8p is associated with leukemic mantle cell lymphoma. Blood. 2001;98:3479-3482.
12. Bea S, Ribas M, Hernandez JM, et al. Increased number of chromosomal imbalances and high-level DNA amplifications in mantle cell lymphoma are associated with blastoid variants. Blood. 1999;93:4365-4374.
13. Bentz M, Plesch A, Bullinger L, et al. t(11;14)-Positive mantle cell lymphomas exhibit complex karyotypes and share similarities with B-cell chronic lymphocytic leukemia. Genes Chromosomes Cancer. 2000;27:285-294.
14. Monni O, Oinonen R, Elonen E, et al. Gain of 3q and deletion of 11q22 are frequent aberrations in mantle cell lymphoma. Genes Chromosomes Cancer. 1998;21:298-307.
15. Lichter P, Joos S, Bentz M, Lampel S. Comparative genomic hybridization: uses and limitations. Semin Hematol. 2000;37:348-357.
16. Jeuken JW, Sprenger SH, Wesseling P. Comparative genomic hybridization: practical guidelines. Diagn Mol Pathol. 2002;11:193-203.
17. Veltman JA, Fridlyand J, Pejavar S, et al. Array-based comparative genomic hybridization for genome-wide screening of DNA copy number in bladder tumors. Cancer Res. 2003;63:2872-2880.
18. Cai WW, Mao JH, Chow CW, et al. Genome-wide detection of chromosomal imbalances in tumors using BAC microarrays. Nat Biotechnol. 2002;20: 393-396.
19. Cheung VG, Nowak N, Jang W, et al. Integration of cytogenetic landmarks into the draft sequence of the human genome. Nature. 2001;409:953-958.
20. Kohlhammer H, Schwaenen C, Wessendorf S, et al. Genomic DNA-chip hybridization in t(11;14)-positive mantle cell lymphomas shows a high frequency of aberrations and allows a refined characterization of consensus regions. Blood. 2004; 104:795-801.
21. DeLeeuw RJ, Davies JJ, Rosenwald A, et al. Comprehensive whole genome array CGH profiling of mantle cell lymphoma model genomes. Hum Mol Genet. 2004;13:1827-1837.
22. Veltman JA, Schoenmakers EF, Eussen BH, et al. High-throughput analysis of subtelomeric chromosome rearrangements by use of array-based comparative genomic hybridization. Am J Hum Genet. 2002;70:1269-1276.
23. Veltman JA, Jonkers Y, Nuijten I, et al. Definition of a critical region on chromosome 18 for congenital aural atresia by arrayCGH. Am J Hum Genet. 2003;72:1578-1584.
24. Zafarana G, Grygalewicz B, Gillis AJ, et al. 12p-Amplicon structure analysis in testicular germ cell tumors of adolescents and adults by array CGH. Oncogene. 2003;22:7695-7701.
25. Vissers LE, de Vries BB, Osoegawa K, et al. Array-based comparative genomic hybridization for the genomewide detection of submicroscopic chromosomal abnormalities. Am J Hum Genet. 2003;73:1261-1270.
26. Eisen MB, Spellman PT, Brown PO, Botstein D. Cluster analysis and display of genome-wide expression patterns. Proc Natl Acad Sci U S A. 1998;95:14863-14868.
27. Sebat J, Lakshmi B, Troge J, et al. Large-scale copy number polymorphism in the human genome. Science. 2004;305:525-528.
28. Iafrate AJ, Feuk L, Rivera MN, et al. Detection of large-scale variation in the human genome. Nat Genet. 2004;36:949-951.
29. Schaffner C, Idler I, Stilgenbauer S, Dohner H, Lichter P. Mantle cell lymphoma is characterized by inactivation of the ATM gene. Proc Natl Acad Sci U S A. 2000;97:2773-2778.
30. Stilgenbauer S, Winkler D, Ott G, et al. Molecular characterization of 11q deletions points to a pathogenic role of the ATM gene in mantle cell lymphoma. Blood. 1999;94:3262-3264.
31. Hirota S, Isozaki K, Moriyama Y, et al. Gain-of-function mutations of c-kit in human gastrointestinal stromal tumors. Science. 1998;279:577-580.
32. Knuutila S, Bjorkqvist AM, Autio K, et al. DNA copy number amplifications in human neoplasms: review of comparative genomic hybridization studies. Am J Pathol. 1998;152:1107-1123.
33. Yu W, Inoue J, Imoto I, et al. GPC5 is a possible target for the 13q31-q32 amplification detected in lymphoma cell lines. J Hum Genet. 2003;48:331-335.
34. Garkavtsev I, Kazarov A, Gudkov A, Riabowol K. Suppression of the novel growth inhibitor p33ING1 promotes neoplastic transformation. Nat Genet. 1996;14:415-420.
35. Ohmori M, Nagai M, Tasaka T, et al. Decreased expression of p33ING1 mRNA in lymphoid malignancies. Am J Hematol. 1999;62:118-119.